

Rat Model of Brain Injury to Occupants of Vehicles Targeted by Land Mines: Mitigation by Elastomeric Frame Designs

Flaubert Tchanchou,¹ Adam A. Puche,² Ulrich Leiste,³ William Fourney,³ Thomas A. Blanpied,⁴ and Gary Fiskum¹

Abstract

Many victims of blast traumatic brain injury (TBI) are occupants of vehicles targeted by land mines. A rat model of under-vehicle blast TBI was used to test the hypothesis that the ensuing neuropathology and altered behavior are mitigated by vehicle frame designs that dramatically reduce blast-induced acceleration (G force). Male rats were restrained on an aluminum platform that was accelerated vertically at up to 2850g, in response to detonation of an explosive positioned under a second platform in contact with the top via different structures. The presence of elastomeric, polyurea-coated aluminum cylinders between the platforms reduced acceleration by 80% to 550g compared with 2350g with uncoated cylinders. Moreover, 67% of rats exposed to 2850g, and 20% of those exposed to 2350g died immediately after blast, whereas all rats subjected to 550g blast survived. Assays for working memory (Y maze) and anxiety (Plus maze) were conducted for up to 28 days. Rats were euthanized at 24 h or 29 days, and their brains were used for histopathology and neurochemical measurements. Rats exposed to 2350g blasts exhibited increased cleaved caspase-3 immunoreactive neurons in the hippocampus. There was also increased vascular immunoglobulin (Ig)G effusion and F4/80 immunopositive macrophages/microglia. Blast exposure reduced hippocampal levels of synaptic proteins Bassoon and Homer-1, which were associated with impaired performance in the Y maze and the Plus maze tests. These changes observed after 2350g blasts were reduced or eliminated with the use of polyurea-coated cylinders. Such advances in vehicle designs should aid in the development of the next generation of blast-resistant vehicles.

Keywords: acceleration; blast; blood–brain barrier; inflammation; synapses

Introduction

EXPOSURE TO BLASTS has resulted in traumatic brain injury (TBI) to >250,000 United States military personnel during the past 10 years. Many of these were occupants in vehicles targeted by land mines and improvised explosive devices (IEDs). Although there are many animal models of blast TBI, most are designed to primarily replicate the effects of blast-induced barometric pressure changes, also known as “overpressure,” on the brain and other organs. Individuals present in vehicles targeted by underbody explosions experience far less change in barometric pressure because of transmission of the most force to the bottom of the vehicle. This energy transduction results in extreme acceleration of the vehicle and its occupants, reaching G forces in the range of 300–3000g.¹

We developed a small-scale model of under-vehicle explosions and used this model to describe how different frame designs, including the double V-shaped hull, affect the loads imparted from an

explosive onto the vehicle. The double V-shaped hull was subsequently incorporated into the mine-resistant, armor protected (MRAP) United States military vehicles in 2007.² During the year prior to this transformation, the fatality rate for exposure to under-vehicle blasts was 60%. As the number of MRAPs deployed to combat zones rose steadily to >10,000 by the end of December 2008, the fatality rate dropped to <10%.³ Most of this improvement in survival was the result of a dramatic reduction in penetrance of the explosions through vehicle hulls into the cabins. Although this was a tremendous achievement, many of those present in the targeted vehicles sustained severe, albeit survivable, injuries, including TBI.

Considering the lack of animal models for TBI experienced by those present in blast-targeted vehicles, we initially developed a model that used anesthetized rats exposed to under-vehicle blasts that generated acceleration G forces in the range of 30–50g.⁴ This force range resulted in histological evidence of axonal damage, but no evidence of change in neurobehavioral measurements. When the

¹Department of Anesthesiology and the Center for Shock, Trauma, and Anesthesiology Research (STAR), and Departments of ²Anatomy and Neurobiology and ⁴Physiology, University of Maryland School of Medicine, Baltimore, Maryland.

³Department of Aerospace Engineering, University of Maryland School of Engineering, Baltimore, Maryland.

force was elevated to 100g, we obtained strong quantitative verification of axonal injury and indications of vestibulomotor alterations.⁵ These experiments were followed by a G-force dose escalation study performed with awake rats present in restraints secured to the top of an aluminum platform that was accelerated vertically at up to 2850g, in response to the detonation of a small explosive positioned under a second, bottom platform. Seventy percent of rats exposed to 2850g died soon thereafter, whereas all rats exposed to 2400g survived, but demonstrated evidence for a transient deficit in working memory, chronic anxiety, and neuropathology.⁶ In these experiments, only a thin, 0.6 cm rubber pad was located between the top and bottom platforms, which dampened oscillations, but had no significant effect on the maximum transmission of force between the two plates.

The current study used this same model of under-vehicle blast TBI to test the hypothesis that the neuropathology and altered behavior that ensue can be mitigated by vehicle frame designs that dramatically reduce the acceleration experienced by the rats. Specifically, we tested the effectiveness of the presence of uncoated and polyurea-coated crushable aluminum cylinders within the chassis at reducing maximum G force, mortality, neuropathology, and neurological injury following exposure to under-vehicle blasts.

Methods

Animals and housing

All animal protocols were approved by the University of Maryland, Baltimore, Animal Use and Care Committee (IACUC) and the United States Army Animal Care and Use Review Office (ACURO). Male Sprague–Dawley rats (300–350g; Envigo, CA), were maintained under a controlled environment with an ambient temperature of $23 \pm 2^\circ\text{C}$, at 12 h light/dark cycle, and continuous access to food and water *ad libitum*. Experimental groups consisted of 10–15 rats/group for behavioral studies and 5–6 rats/group for immunohistochemistry or biochemical analyses.

Underbody blast and blast mitigation design

Following scaling analysis and procedures previously described,^{4,7} rats were exposed to underbody blast paradigms generating a mean maximal G force of $\sim 2850\text{g}$, as recently reported.⁶ In brief, two isoflurane anesthetized rats were secured, while unconscious, within fiberglass restrainers (Stoeling Inc., IL) bolted to the top aluminum platform, which was 38 cm^2 and 2.5 cm thick. The restraints included a custom-fit metallic cone to minimize head movement, secondary acceleration, and head impact. The top platform was located directly above another 38 cm^2 aluminum platform, which was 5.0 cm thick. Both platforms were separated by a 0.6 cm thick, hard-rubber pad to dampen oscillatory acceleration forces. Each platform had a 3.5 cm diameter hole located at each corner through which 2.0 cm thick guide-poles were located, allowing for purely vertical movement. This device was located in a steel water tank at a water level of 0.2 cm below the bottom platform. An explosive charge of 2.0 g pentaerythritol tetranitrate (PETN) was secured at a fixed 5 cm depth (stand-off distance) in the water beneath the center of the lower platform. This charge was detonated electrically exactly 5 min after anesthesia was discontinued, when the rats were fully conscious.

Experiments were performed to test the ability of unique, acceleration absorbing frame designs to reduce the G force transmitted to the rats. Five uncoated or polyurea-coated, crushable aluminum cylinders were placed between the top and bottom platforms in an effort to mitigate the force transduction between the bottom and top platforms. Each cylinder was 66 mm wide and 38 mm high, with an aluminum wall thickness of 0.1 mm. When present, the polyurea

coating thickness was 1.6 mm thick. The weight of each cylinder was 2.1 g for the uncoated and 14.6 g for the polyurea coated. For all blast paradigms, with or without mitigation, two accelerometers were placed on the top of the higher platform near the head end of the restraints and used to determine the acceleration and jerk (first derivative of acceleration), measured by Underwater Explosives Research Division (UERD)-Tools software (United States Navy). Pressure sensors were also placed near the head-end of the restraints during several experiments, verifying that the pressure changes experienced by the rats were $<1\text{ psi}$. Sham animals were also anesthetized with 4% isoflurane for 5 min, secured on the platform, and removed 5 min later without blast exposure.

All blast and sham animals were returned to their respective cages immediately after blast or sham procedures and examined for any physical injuries every 30 min for 3 h. Necropsies were performed immediately on all animals that died following blast exposure.

Behavioral analysis

The Y maze test was performed to assess hippocampus-dependent working memory on day 0, at $\sim 1\text{ h}$, and at days 6, 13, and 27 post-injury, as previously described.^{6,8} In brief, each rat was placed at the center of the maze and allowed to explore for 5 min. Movement was recorded using an overhead camera, and analysis was performed with the Any-Maze software (SD instruments, CA). Arm visit sequences and number of entries to each arm were recorded. Working memory was defined by the frequency of alternately exploring different arms, and was determined using the formula: total number of alternations/(total number of arm entries -2) $\times 100$. The elevated Plus maze test was performed to evaluate anxiety-like behaviors by rats on days 1, 8, 14, and 28 post-blast, as previously described.^{6,9} In brief, rats were individually placed on the central area of the Plus maze and allowed to explore for 10 min. Movement was recorded by an overhead camera, and data were analyzed by Any-maze software, to provide information including the time spent in each arm and the central area and the total distance traveled. Anxiety-like behavior is inversely proportional to the time the rats spend in the open arms.

Experimental time points, tissue collection, and processing

Rats were deeply anesthetized with an intraperitoneal (i.p.) injection of a mixture of ketamine (160 mg/kg) and xylazine (120 mg/kg) at different times following blast or sham blast procedures (Fig. 1). They were then euthanized by exsanguination via transcardial perfusion for 5 min with oxygenated artificial cerebrospinal fluid containing 148 mM NaCl, 5 mM glucose, 3.0 mM KCl, 1.85 mM CaCl_2 , 1.7 mM MgCl_2 , 1.5 mM Na_2HPO_4 , and 0.14 mM NaH_2PO_4 (pH 7.4). The rats were then perfused for 15 min with a fixative containing 4% paraformaldehyde in 50 mM K_2HPO_4 and 50 mM KH_2PO_4 (pH 7.4). Their brains were removed, maintained in fixative for 24 h, and transferred to 30% sucrose. After brains sank to the bottom of the 30% sucrose solution within a few days, they were individually sliced in $40\ \mu\text{m}$ thick sections, preserved in cryoprotectant (66 mM NaH_2PO_4 , 190 mM Na_2HPO_4 , 0.87 M sucrose, 30% ethylene glycol, and 1.25 mM povidone), and stored for histology and immunohistochemistry at -20°C . For Western blot analysis, rats were decapitated with a guillotine. Their brains were rapidly removed and dissected to collect different regions, including the hippocampus and the cortex, which were immediately frozen on dry ice and stored at -80°C .

Immunostaining

Histological staining of frozen coronal brain sections was performed to assess the level of perivascular immunoglobulin G (IgG) effusion as a measure of blood–brain-barrier (BBB) disruption. These sections were also used for immunostaining of the vascular

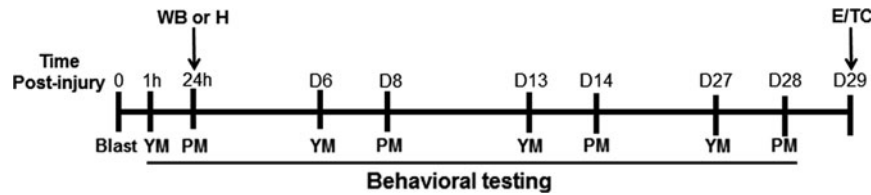


FIG. 1. Experimental design. Detailed timeline of behavioral tests and end-points of experimental procedures starting on study day 0 (blast or sham blast exposure). YM, Y-maze test; PM, plus-maze test; H, histology; WB, Western blots; E, euthanasia; TC, tissue collection.

endothelial marker glucose transporter 1 (GluT-1) and the intercellular adhesion molecule 1 (ICAM-1). We also assessed the presence of inflammatory cells by co-immunostaining for F4/80 (marker of activated microglia/macrophages) and inducible nitric oxide synthase (iNOS). Further, we stained for the expression of apoptosis biomarker, cleaved caspase 3, and the density of pre- and post-synaptic markers Bassoon and Homer-1, respectively. Staining methods used were either fluorescence immunostaining or nickel diaminobenzadine (DAB) immunostaining. Brain sections were co-stained for the expression of ICAM-1 and GluT-1, F4/80 and iNOS, Bassoon and Homer-1, or cleaved caspase 3 and neuronal nuclear antigen as previously described.¹⁰ In brief, free-floating sections were rinsed in phosphate buffered saline (PBS) and then blocked in 1% horse serum in PBS containing 0.3% Triton X for 1 h. Sections were transferred in a solution containing goat anti-ICAM-1 antibody (1:2000; Santa Cruz, CA) and mouse anti-glucose transporter monoclonal antibody (1:1500; Abcam, MA), rabbit anti-cleaved caspase-3 polyclonal antibody (1:10,000; Millipore, CA) and mouse anti-NeuN monoclonal antibody clone, A60 (1:2000; Millipore, CA), rat anti-F4/80 monoclonal antibody (1:500; eBioscience, San Diego, CA) and rabbit anti-iNOS polyclonal antibody (1:3000; Millipore, CA), or mouse anti-Bassoon (1:2000; Enzo life sciences, NY) and rabbit anti-Homer-1 antibody (1:1000; Invitrogen/ThermoFisher Scientific, NY) and incubated overnight at 4°C. They were washed in PBS and incubated for 1 h at room temperature in a mixture of corresponding secondary antibodies Alexa Fluor 488 or Alexa Fluor 594 (1:1500; Invitrogen, NY). Sections were washed with PBS followed by 4',6-diamidino-2-phenylindole (DAPI) used for nuclei counterstaining.

Brain sections were single-labeled for the presence of IgG, using nickel DAB. Free-floating sections were rinsed in PBS, blocked with 1% horse serum, and incubated with rabbit IgG antibody (1:2500; eBioscience, CA) overnight at 4°C. Sections were washed and incubated at room temperature in biotinylated goat anti-rabbit secondary antibody (1:2000; Vector Laboratories Inc., CA), for 1 h, followed by incubation in Vesta Stain solution and in nickel DAB, and rinsed in PBS.

Western blot analysis

Western blotting analysis was used to evaluate the expression levels of the extracellular signal-regulated kinase 1/2 (ERK-1/2), phosphorylated ERK, B-cell lymphoma 2 (Bcl-2), α ii spectrin and β -actin proteins in the hippocampus of blast and sham rats. Hippocampal tissues were manually homogenized in lysis buffer composed of 50 mM HEPES (pH 7.5), 6 mM $MgCl_2$, 1 mM ethylenediaminetetraacetic acid (EDTA), 75 mM sucrose, 1 mM dithiothreitol, 1% Triton X-100 (Sigma, MO), and 1% protease/phosphatase inhibitor cocktail (Cell Signaling Technology, MA). Homogenates were centrifuged at 10,000g for 20 min. Proteins (20–40 μ g) present in the supernatants were separated by electrophoresis on 4–12% SDS-polyacrylamide gels (Bio-rad, CA), and then transferred to a nitrocellulose membrane. Membranes were blocked with 1% bovine serum albumin (BSA) and incubated overnight at 4°C with rabbit polyclonal antibodies against ERK1/2,

phosphor-ERK1/2 (1:1000; Cell Signaling Technology, MA), α ii spectrin (1:3000, Invitrogen/ThermoFisher scientific, NY), Bcl-2 (1:2000, ProteinTech, IL) and mouse monoclonal antibody against β -actin (1:4000; Sigma, MO). Blots were washed in Tris-buffered saline with 0.1% Tween 20 and incubated for 1 h at room temperature with corresponding horseradish peroxidase (HRP)-conjugated secondary antibodies (1: 5000; Millipore, MA). HRP-labeled proteins were detected by enhanced chemiluminescence (ECL, Thermo Scientific, IL), and protein bands were visualized using a digital blot scanner (LI-COR, NE).

Data analysis

The number of cleaved caspase 3 immunopositive cells were quantified using 40 μ m thick sections of the hippocampus dentate gyrus and cornu ammonis (CA) 2/3 regions by the optical fractionator method of stereology using the Stereo Investigator software (MBF Bioscience, VT). For each brain, six sections corresponding to every 12 serial sections expanding from bregma -1.60 to -6.3 to cover the whole hippocampus area were analyzed. For quantification, the dentate gyrus and the (CA 2/3) subregions in the hippocampus of each brain hemisphere were demarcated. Grid spacing of 75 μ m \times 75 μ m in the x and y -axis and guard zones of 2 μ m at the top and bottom of each section were used to count immunopositive cell bodies. The total number of cleaved caspase 3 positive cells in the hippocampal subregion of interest was divided by the covered area to determine the cellular density per area, expressed as cells/mm².

ImageJ software (National Institutes of Health [NIH]) was used to measure immunoblot protein band signal intensity and the percent area of IgG, ICAM-1, or F4/80 immunostaining in brain tissue. The signal intensities for Bcl-2 and α ii spectrin were expressed as a ratio of β actin signal intensity (used as loading control) and that of phospho-ERK1/2 was expressed as a ratio of total ERK1/2. Sections stained for IgG, ICAM-1, or F4/80 were optically segmented by threshold. These thresholded images were automatically measured for the relative percent containing a positive IgG, ICAM-1, or F4/80 signal in ImageJ. This method is proportional to the percent area covered by the IgG, ICAM-1, or F4/80 immunopositive signal.

The puncta analyzer software was generously provided by Dr. Cagla Eroglu (Duke University Medical Center, Durham, NC) and incorporated in ImageJ to determine the Bassoon, Homer-1, and Bassoon/Homer-1 co-localized puncta as previously described.^{11,12} In brief, sections co-immunostained against Bassoon and Homer-1 were highlighted, and quantification was performed with rolling ball radius set at 50 with “white background” unchecked and the puncta size for Bassoon and Homer-1 set at 4 pixels. At the end of the quantification, the puncta density for Bassoon and Homer-1 and the co-localized Bassoon/Homer-1 puncta were generated.

Statistical analysis

Statistical analyses were performed using GraphPad InStat 3 software (GraphPad Software, Inc., La Jolla, CA). Analysis of variance together with Tukey–Kramer multiple comparisons post-hoc test were used to compare differences among the multiple

groups. Results are expressed as mean \pm standard error of the mean (SEM). Statistical significance was defined as $p < 0.05$.

The individuals who performed the histological, biochemical, and behavioral assays were blinded to animal group identifications, using codes that were revealed after data collection was completed.

Results

Mitigation of under-vehicle, blast-induced mortality

We previously reported that exposure of rats to 2400g acceleration during an under-vehicle blast scenario caused significant neuropathology and neurobehavioral deficits, whereas exposure to 2850g resulted in 67% acute mortality.⁶ Moreover, when the peak acceleration was reduced to 1200g by reducing the size of the explosive, there were less neuropathology and fewer neurobehavioral deficits. In this study, we used the same basic model to determine if different vehicle frame designs could be used to mitigate the acceleration experienced by the rats, and, therefore, reduce TBI.

Table 1 provides a comparison of the maximal acceleration G force, the rate of change in acceleration (jerk), and the incidence of mortality for rats subjected to under-vehicle blasts using three different vehicle designs. The previously reported experiments that generated 2850g were performed using a thin rubber pad (0.6 cm) placed between the bottom aluminum plate located above the explosive and the top plate on which the rats were restrained. In an attempt to reduce the G force transmitted to the rats, we placed five crushable aluminum cylinders between the two plates, with one located at each of the four corners and one located in the center. Under these conditions and using the same blast parameters that generated 2850g in the absence of cylinders, all five cylinders were completely crushed or compressed to $\sim 10\%$ of their original height. There was a small but statistically insignificant 18% reduction in maximal G and a 15% reduction in jerk, in comparison with the values obtained in the absence of inter-plate cylinders. Nevertheless, presence of these cylinders reduced the mortality rate from 67% to 20%.

We then tested the hypothesis that coating the cylinders with polyurea would reduce mortality even further by reducing both the maximal G force and the jerk. Polyurea is an elastomer commonly used in truck bed liners. Polyurea is compressible and rebounds following compression, resulting in an excellent ability to absorb energy in the form of acceleration.² The presence of five polyurea-coated cylinders between the two aluminum plates resulted in a highly significant ($p < 0.01$) 80% reduction in maximal acceleration and a 57% reduction in jerk. There were no deaths among 24 rats used in the experiments employing the polyurea-coated cylinders (Table 1).

TABLE 1. SUMMARY OF THE EFFECTS OF ELASTOMERIC FRAME DESIGN ON BLAST-INDUCED ACCELERATION G FORCE, JERK, AND MORTALITY

Vehicle design	G force	Jerk ^a	Mortality
No mitigation ^b	2851 \pm 359	1.77 \pm 0.33	4/6 (67%)
Uncoated cylinders	2331 \pm 128	1.51 \pm 0.27	4/20 (20%)
Polyurea-coated cylinders	536 \pm 46	0.76 \pm 0.11	0/24 (0%)

^aJerk is the first derivative of acceleration (G force) and the second derivative of velocity, and is expressed as $\times 10^{13}$ meter⁻³.

^bThe acceleration data and survival outcomes obtained from experiments using simulated vehicles with no G force mitigation were published previously.⁶

Acceleration mitigation improves behavioral outcomes

The ability of different vehicle designs to mitigate blast-induced behavioral deficits was tested using the Y maze, for working memory, and the elevated Plus maze, for anxiety, at different times up to 4 weeks following blast exposure (Fig. 2). All animals were tested with the Y maze at 1 h following exposure to the under-vehicle blast and again at 6, 13, and 27 days. In comparison with shams, at day 0, the percent of spontaneous alternation among the three arms of the maze was substantially lower for rats that were exposed to the blasts using simulated vehicles that included uncoated cylinders ($0.9 \pm 0.7\%$; $n = 8$) than the percent of alternation for shams ($27 \pm 12\%$; $p < 0.001$; $n = 10$) or for rats secured to the

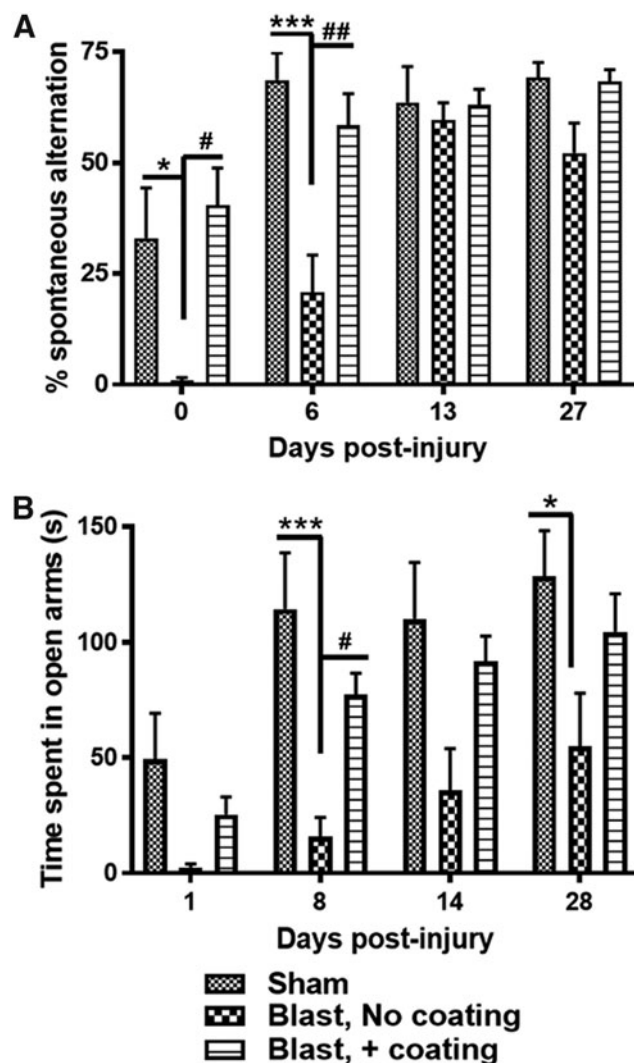


FIG. 2. Coating of cylinders with polyurea is necessary for mitigation of behavioral deficits following under-vehicle blast. Rats were restrained on the top of a simulated vehicle that incorporated either uncoated or polyurea-coated aluminum cylinders, resulting in maximal acceleration of 2350g and 550g, respectively. (A) Polyurea-coated cylinders protected rats from loss of spontaneous alternation in the Y maze at day 0 ($^{*}\#p < 0.05$, $^{###}p < 0.01$; $n = 10-16$) and at day 6 ($^{##}p < 0.01$, $^{***}p < 0.001$). (B) Polyurea-coated cylinders were also effective at protecting against anxiety behavior, which was inversely related to the time rats spent in the open arms of the elevated Plus maze. ($^{***}p < 0.001$, $^{#}p < 0.05$, $^{*}p < 0.05$; $n = 10-16$).

simulated vehicle that included polyurea-coated cylinders ($40 \pm 8\%$; $p < 0.01$; $n = 16$). By day 6, the percent of spontaneous alternation for shams rose to $68 \pm 12\%$, which was significantly greater than the score for shams at day 0 ($p < 0.001$). The score for animals used for the uncoated cylinder blast paradigm also rose significantly to $37 \pm 7\%$ in comparison with the score at day 0 ($p < 0.001$). Nevertheless, this score was still much lower than the score for either the shams (68 ± 6 ; $p < 0.01$) or for rats that were exposed to the blast in simulated vehicles equipped with polyurea-coated cylinders (58 ± 7 ; $p < 0.005$). By days 13 and 27, there were no significant differences among the three animal groups.

Similar patterns of behavioral injury were observed among the three animal groups over 28 days post-blast using the elevated Plus maze test for anxiety. There were no significant differences in the time spent in the open arms of the Plus maze among the animal groups at 1 day following the blast, although there was a trend toward the shortest time for rats used with the uncoated cylinder vehicle design. On day 8, the time in open arms (16 ± 8 sec) was much lower in these same rats compared with shams (115 ± 22 sec; $p < 0.001$) or with rats that were used with the uncoated cylinder vehicle (77 ± 9 sec; $p < 0.05$). There were no significant differences among groups at day 14 following blasts; however, there was still a trend toward lower time for the rats used with the uncoated cylinder vehicles. At day 28 post-blast, the time spent in open arms by rats in the uncoated cylinder animal group (51 ± 22 sec) was significantly lower than that of shams (130 ± 21 sec; $p < 0.05$). The rats in the polyurea-coated cylinder animal groups exhibited time in open arms of 100 ± 20 sec, which was not different from shams.

These behavioral assays were also applied to the two rats that survived the blasts that generated 2850g, where no cylinders were present between the two platforms. Neither of these rats spent any

time in the open arms of the Plus maze on days 1 and 8 post-injury, and they spent just an average of 42 sec on day 28 (not shown). Moreover, neither rat exhibited any successful alternation between Y maze arms when tested 1 h after blast, and they exhibited an average of only 38% on days 6 and 13 post-blast. However, these rats exhibited an average of 68% spontaneous alternations on day 27 compared with $69 \pm 3\%$ for sham rats.

Mitigation of acceleration reduces cerebrovascular damage caused by under-vehicle blasts

We recently reported that under-vehicle blasts generating either 1200g or 2400g acceleration force reduced the expression of tight junction proteins occludin and zona occludens 1 (ZO-1) in the rat hippocampus and cortex.⁶ This reduction in tight junction proteins was accompanied by increased expression of von Willebrand factor (vwf), a marker of cerebrovascular endothelial damage,⁶ suggesting a disruption of BBB integrity. In the current study, rat brain sections were immunostained for IgG at 24 h post-blast to detect extravasation from the vasculature into the parenchyma, indicative of compromised BBB (Fig. 3). The area of IgG immunostaining in the cortex was 140% greater for rats exposed to the blast paradigm with uncoated cylinders ($5.7 \pm 0.7\%$) than for sham animals ($2.4 \pm 0.2\%$; $p < 0.01$; $n = 5-6$) and 95% greater for rats exposed to the blast paradigm that incorporated polyurea-coated cylinders ($3.1 \pm 0.4\%$; $p < 0.05$; Fig. 3A,B). In addition, exposure to an under-vehicle blast resulted in an increase in ICAM-1 immunoreactivity, which is a marker of leucocyte infiltration into the parenchyma (Fig. 4A,B).^{13,14} The area of ICAM-1 immunoreactivity ($6.7 \pm 1.8\%$) in the cortex of rats after blasts using uncoated cylinders was significantly higher than that of shams ($0.9 \pm 0.3\%$; $p < 0.01$). ICAM-1 levels were partially

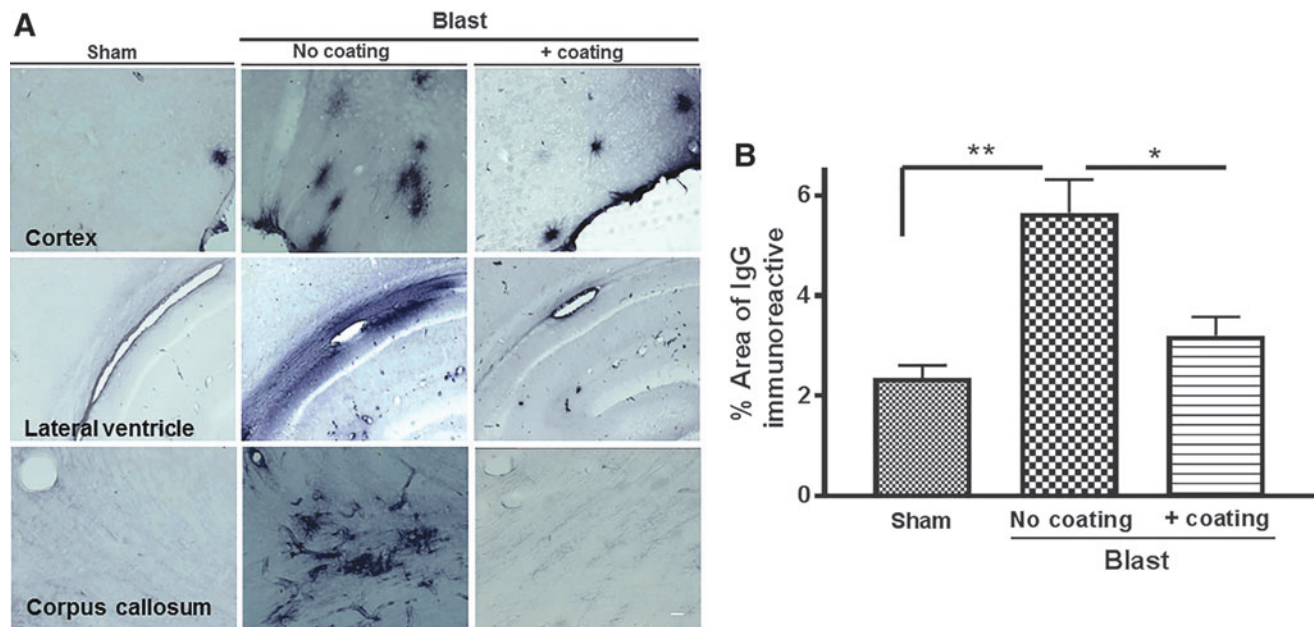


FIG. 3. Increased perivascular immunoglobulin (IgG) effusion in the brain post-blast and by incorporation of polyurea-coated cylinders. (A) Representative microscopic images exhibiting IgG immunoreactivity in different brain regions at 24 h post-blast or post-sham blast. Scale bar is 50 μ m. (B) Quantification of the percentage of the cerebral cortex area that was immunopositive for IgG. There was a significant, 700% increase in rat cortical IgG immunostaining following blasts generating 2300g compared with sham animals (** $p < 0.01$, $n = 5$) and a 100% increase compared with the area present following blasts with vehicles that incorporated polyurea-coated cylinders (* $p < 0.05$; $n = 6$).

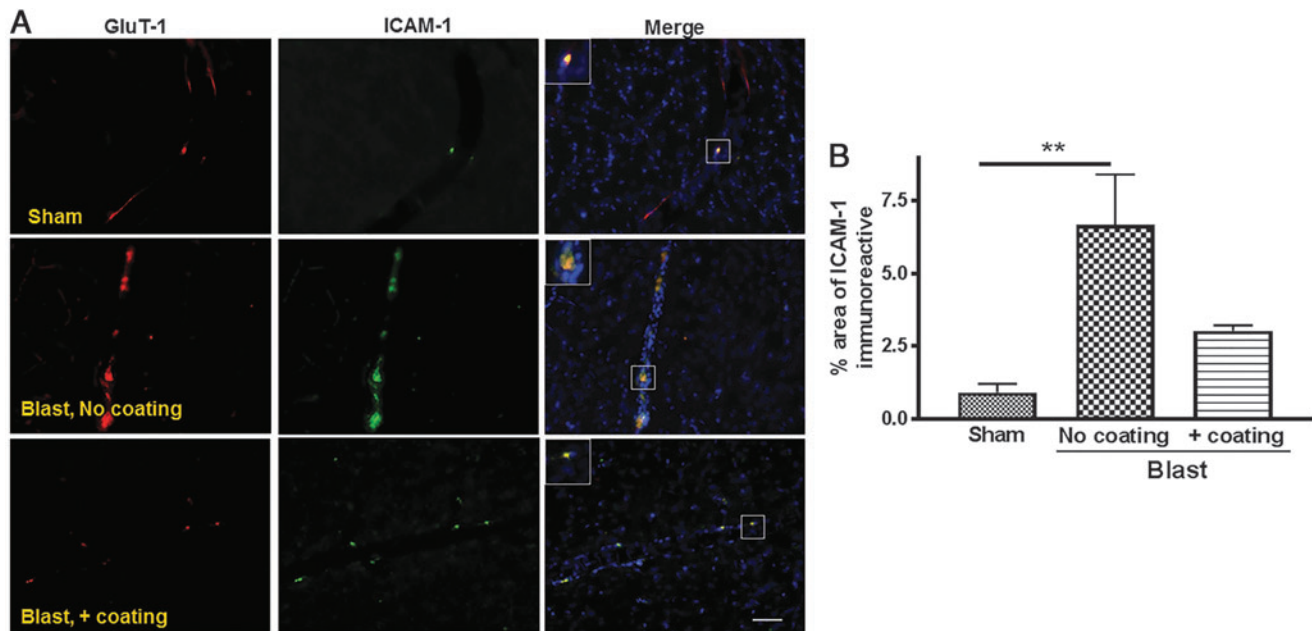


FIG. 4. Increased intercellular adhesion molecule 1 (ICAM-1) expression in the brain following under-vehicle blast and mitigation by incorporation of polyurea-coated cylinders. **(A)** Representative microscopic images expression of ICAM-1 (green) and glucose transporter 1 (GluT-1) (red) in immunostained rat brain sections at 24h post-blast. Size bar is 100 μ m. **(B)** Quantification of the area of ICAM-1 immunoreactivity indicating significantly increased levels of ICAM-1 in the brains ($n=5$) of rats subjected to blast intensity with incorporation of uncoated cylinders compared with shams (** $p < 0.01$; $n=6$). ICAM-1 immunostaining was not significantly different between shams and after blasts that incorporated the polyurea-coated cylinders.

reduced by blasts conducted under vehicles that included the polyurea-coated cylinders ($3.0 \pm 0.2\%$). The inserts in all images represent 4 \times magnification of the boxed area to provide a better view of the co-localized proteins.

Mitigation of acceleration reduces cellular inflammatory reactions

Inflammation is an important hallmark of brain injury in both animal models and TBI patients.^{6,15,16} We observed that rats subjected to the lethal blast intensity in simulated vehicles that contained cylinders that were not coated with polyurea exhibited substantially higher iNOS and F4/80 co-expressing microglia/macrophages covering $13.0 \pm 3.4\%$ of these animal brains than did shams ($1.5 \pm 0.1\%$, $p < 0.01$; $n=5-6$). In contrast, the presence of polyurea-coated cylinders significantly prevented microglia/macrophages infiltration, reducing populated brain area to $4.8 \pm 1.0\%$ ($p < 0.05$; $n=5-6$) (Fig. 5. A,B).

Mitigation of acceleration reduces loss of hippocampal synaptic densities

A reduction in the levels of synaptic proteins has been demonstrated in animals and humans following impact and blast TBI.^{6,17,18} Considering the important roles that the hippocampus plays in cognition and memory, we tested for the effects of blast-induced acceleration on the density of the pre-synaptic protein, Bassoon, and the post-synaptic protein, Homer-1 in the hippocampus dentate gyrus subgranular layer (SGL) and in the (CA2) subregion. Rats exposed to the lethal blast paradigm that included only uncoated cylinders in the frame design exhibited a 25% decrease in the SGL Bassoon puncta ($p < 0.05$; $n=5-6$) (Fig. 6 A,B) and a 46% reduction in Homer-1 puncta ($p < 0.01$, Fig. 6B), resulting in 44% reduced co-localized Bassoon/Homer-1 puncta

($p < 0.05$, Fig.6 A,B), compared with sham animals. Overall, the interaction between pre-synaptic marker Bassoon and post-synaptic marker Homer-1 in the SGL gyrus indicated 26% greater bassoon puncta co-localization in the SGL of sham rats than in rats exposed to the lethal blast paradigm with uncoated cylinders. However, there was no significant change in the fraction of co-localized Homer-1 between sham and blast rats following experiments conducted in the presence of polyurea-coated cylinders, suggesting an overall loss of synapses in the hippocampus SGL (Fig. 6C). In addition to synaptic changes occurring in the dentate gyrus-SGL, we also observed that Homer-1 puncta intensity in the CA2 region of the hippocampus was reduced by 41% following experiments using uncoated cylinders compared with shams ($p < 0.01$, Fig. 7B). No significant difference in Bassoon puncta density was found between rats in those groups (Fig. 7B). However, the decrease in Homer-1 puncta was associated with a 38% reduction in Bassoon/Homer-1 puncta co-localization in the CA2 of rats subjected to blast with uncoated cylinders, compared with shams ($p < 0.05$, Fig. 7B) and a 39% decrease in co-localized Bassoon fraction, again suggesting an overall loss in synapses in the CA2 of these blast animals (Fig. 7C).

The incorporation of polyurea-coated cylinders prevented the loss in Bassoon and Homer-1 puncta in the hippocampus SGL by 10% and 34% ($p < 0.05$, Fig. 6B), respectively, in comparison with the immunopositive puncta present in the SGL observed after blasts in the presence of uncoated cylinders. Moreover, this substantial protection of the post-synaptic marker Homer-1 in the SGL of these rats resulted in a 42% increase in co-localized Bassoon/Homer-1 and 29% more co-localized Bassoon fraction compared with rats exposed to blast with no coated cylinders ($p < 0.05$, Fig. 6B,C). In addition, the presence of polyurea-coated vehicles reduced the loss in Homer-1 puncta in the CA2 region by 12% versus rats exposed to blasts with uncoated cylinders. This protection of Homer-1 puncta in the CA2 region was associated with a 28% increase in Bassoon/

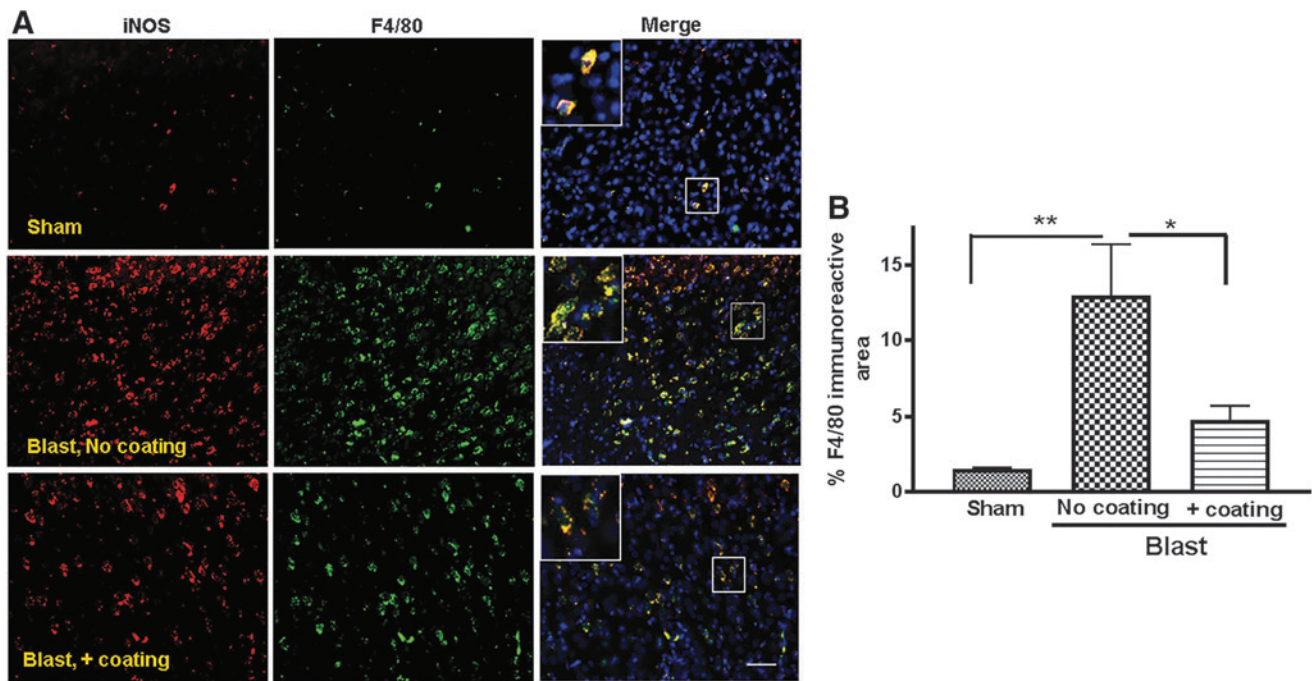


FIG. 5. Activated microglia/microphages following under-vehicle blasts and mitigation by incorporation of polyurea coated cylinders. (A) Representative fluorescent images of F4/80 immunopositive cells (green) showing overlap with inducible nitric oxide synthase (iNOS) immunopositive cells (red) and 4',6-diamidino-2-phenylindole (DAPI) as counterstain (blue). Scale bar is 100 μm . (B) Quantification of the F4/80 immunopositive area in the cortex suggests dramatic increase of activated microglia/microphages in the brains of rats subjected to lethal blast intensity with no polyurea coating compared with sham rats ($n=5$; $**p < 0.01$). Levels of activated microglia/microphages were significantly reduced ($n=6$; $*p < 0.05$) in the brains of rats exposed to blast with polyurea coating mitigation system.

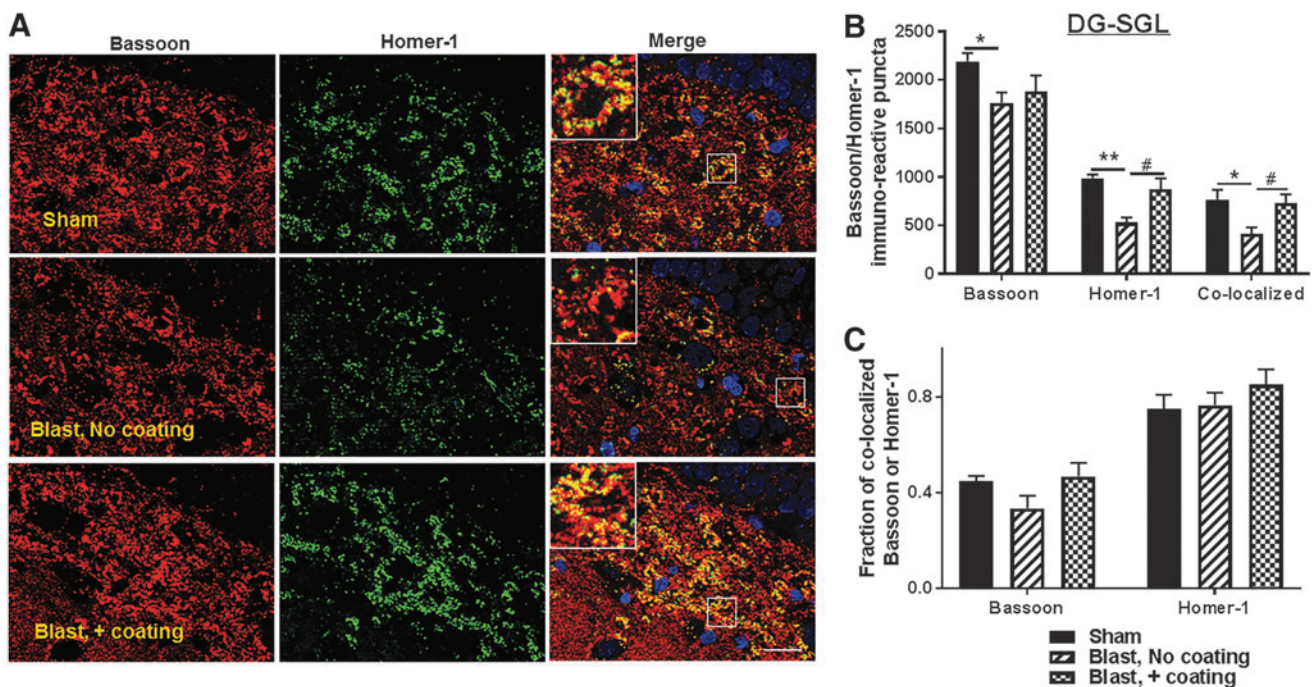


FIG. 6. Synaptic protein density decreased in rat dentate gyrus subgranular layer (SGL) 24 h post-injury, protected by the advanced hull design system. (A) Representative fluorescent images demonstrating the presence of the pre-synaptic protein Bassoon (red) and the post-synaptic protein Homer-1 (green), and 4',6-diamidino-2-phenylindole (DAPI)-stained nuclei in the dentate gyrus SGL of the rat hippocampus. Scale bar is 100 μm . (B) Quantitation of Bassoon, Homer-1, and Bassoon/Homer-1 co-localized puncta density indicated a significant decrease in Homer-1 and Bassoon/Homer-1 co-localized puncta in the SGL of rats exposed to lethal blast intensity with no polyurea coating compared with sham ($n=5$; $*p < 0.05$ and $**p < 0.01$). Blast-induced impairment in synaptic proteins expression was significantly prevented by the polyurea coating mitigation system ($n=6$; $*p < 0.05$).

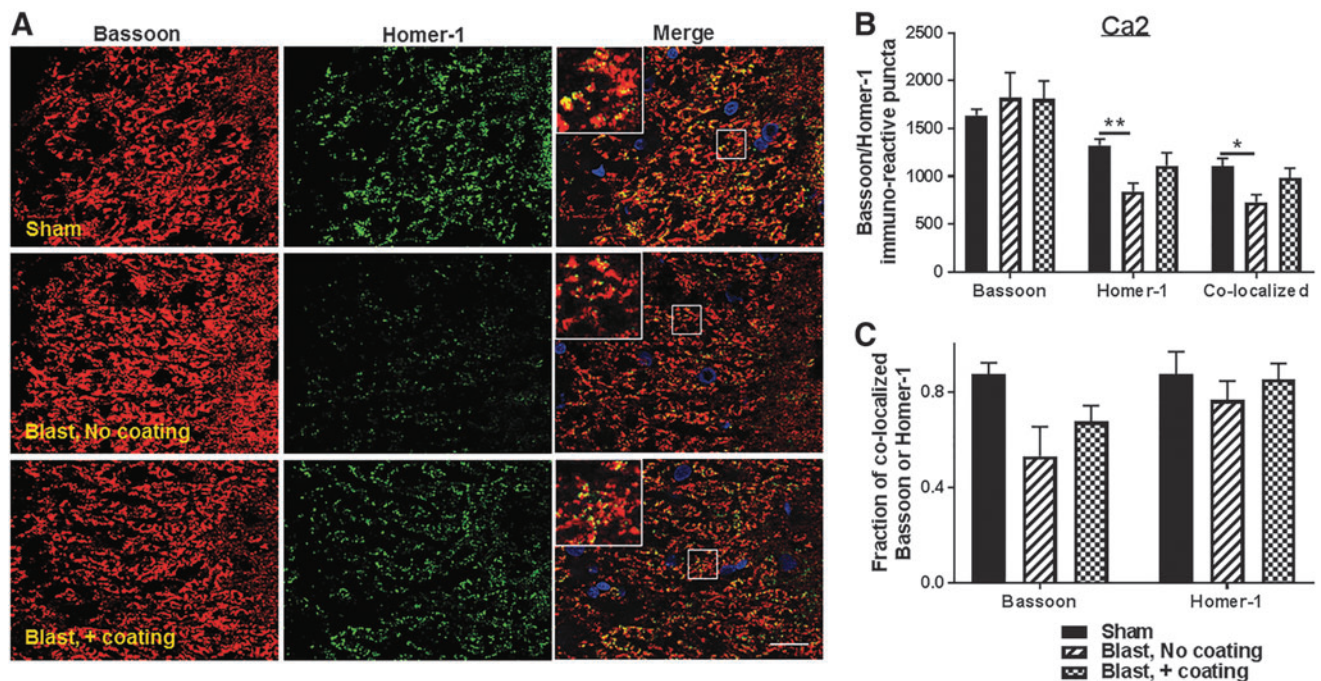


FIG. 7. Synaptic protein density decreased in the rat cornu ammonis (CA)2 region 24 h post-injury, protection by the advanced hull design system. **(A)** Representative fluorescent images demonstrating the presence pre-synaptic protein bassoon (red) and post-synaptic protein Homer-1 (green) and 4',6-diamidino-2-phenylindole (DAPI)-stained nuclei in the CA2 region of the rat hippocampus. Scale bar is 100 μ m. **(B)** Quantitation of Bassoon, Homer-1, and Bassoon/Homer-1 co-localized puncta density indicated a significant decrease in Homer-1 and Bassoon/Homer-1 co-localized puncta in the CA2 region of rats exposed to lethal blast intensity with no polyurea coating compared with sham ($n=5$; $*p<0.05$ and $**p<0.01$). Blast-induced impairment in synaptic proteins expression was relatively prevented by the polyurea coating mitigation system ($n=6$).

Homer-1 co-localized puncta and 11% higher co-localized Bassoon puncta fraction in the same region (Fig. 7C). Taken together, these results indicate that the acceleration mitigation provided by the presence of polyurea-coated cylinders located between the two platforms prevented the loss of synapses both in the hippocampal SGL and CA2 regions.

Mitigation of blast-induced acceleration reduces hippocampal neuronal apoptosis

We recently reported a blast intensity-dependent appearance of cleaved caspase 3 in the hippocampal neurons of rats exposed to blast intensity of 1200g and 2400g force.⁶ In the current study, we observed a significant increase in cleaved caspase 3 immunopositive cells in the dentate gyrus (13.1 ± 2.7 cells/mm²) and CA2/CA3 region (7.8 ± 2.6 cells/mm²) of rats exposed to blasts in the presence of uncoated cylinders, in comparison with shams in the dentate gyrus with 1.5 ± 0.3 cells/mm² ($p<0.01$) and in the CA2/CA3 regions with 1.1 ± 0.2 cells/mm² ($p<0.05$) (Fig. 8B). The polyurea coating mitigation system significantly reduced the presence of cleaved caspase 3 positive cells in the dentate gyrus with 6.3 ± 1.6 cells/mm² ($p<0.05$), and in the CA2/CA3 regions with 4.3 ± 1.0 cells/mm² ($p<0.05$) (Fig. 8B; $n=5-6$).

Mitigation of acceleration with crushable cylinders partially protects against blast-induced ERK dephosphorylation and α ii spectrin proteolysis

Following the observation that exposure to high blast intensity increases hippocampal caspase 3 immunopositive cells, we examined the effect of blasts and mitigation of blast-induced

acceleration on additional apoptosis-related proteins. Our results revealed a 60% decrease in ERK phosphorylation ($p<0.01$; Fig. 9A,C) and a dramatic 75% increase in α ii spectrin proteolytic breakdown products ($p<0.001$; Fig. 9B,E) in rats subjected to under-vehicle blasts in the presence of uncoated cylinders compared with levels observed with sham rats. Importantly, the presence of polyurea-coated cylinders reduced ERK phosphorylation by 50% ($p<0.05$; Fig. 9A,C) and reduced α ii spectrin breakdown products by 60% ($p<0.01$; Fig. 9B,E) compared with levels in the hippocampus of rats exposed to blast with uncoated cylinders. However, the incorporation of polyurea-coated cylinders in the vehicle frame design did not protect against blast-induced reduction in the levels of Bcl-2, an important antiapoptotic protein (Fig. 9A,D).

Discussion

This study is the first to provide neurochemical, histopathological, and behavioral evidence that under-vehicle, blast-induced mortality and TBI in laboratory animals can be mitigated by vehicle design modifications that dramatically reduce the transmission of force from the bottom of the vehicle to where the animals are located. The scaling factor between these small-scale blasts and those full-scale explosions caused by land mines is ~ 10 .¹⁹ Therefore, we estimate that the full-scale blast-induced acceleration of 280g would affect people similarly to how 2850g affected rats. The additional estimation that the G forces transmitted to military vehicles by land mines ranged from 200 to 4000g supports the relevance of the results we reported earlier using adult rats and our small-scale underbody blast model.^{4,6}

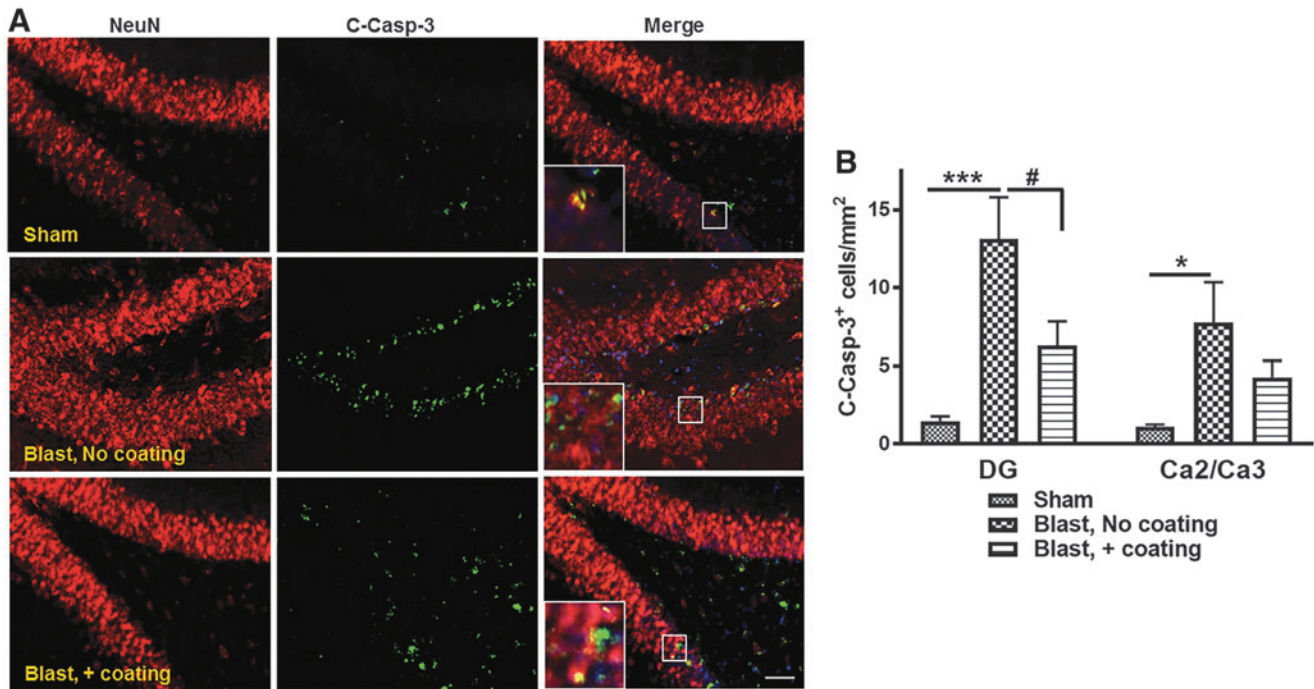


FIG. 8. Cleaved caspase 3 immuno-positive cells present in rat hippocampus. **(A)** Representative fluorescent images showing cleaved caspase 3 immunopositive cells (green) overlapping mostly with NeuN immunoreactive cells (red), and 4',6-diamidino-2-phenylindole (DAPI) for nuclei counterstaining. Scale bar is 100 μm . **(B)** Quantitation indicated significant increase in cleaved caspase 3 immunoreactive cells in the dentate gyrus and cornu ammonis (CA)2/3 region of rats subjected to blast with no polyurea coating compared with sham animals ($n=5$; $*p<0.05$, and $***p<0.001$). The advanced hull design significantly reduced the blast-initiated hippocampal apoptotic cell loss ($n=6$; $\#p<0.05$).

We previously demonstrated that 67% of animals exposed to blast-induced acceleration of 2850g die immediately after the blast exposure, apparently as a result of lung damage.⁶ We therefore applied the settings used in these experiments to test the hypothesis that modifications of vehicle frame design can reduce the G force experienced by the laboratory rats to an extent that increases survival. These settings included the standoff distances from both the explosive and the water line to the bottom of the simulated vehicle and the weight of the PETN explosive that was used. Experiments performed in the absence of animals indicated that G-force mitigation could be detected with our system using aluminum cylinders placed between the top and bottom plates constituting the frame of a vehicle.² The first attempt at mitigating under-vehicle blast-induced mortality utilized the placement of five uncoated aluminum cylinders between the two plates. This modification resulted in a small but nonsignificant reduction in both the maximum G force and the jerk; that is, the rate of change in acceleration (Table 1). Nevertheless, the presence of these collapsible structures resulted in a robust 80% reduction in mortality compared with the two thirds that died following blasts in the absence of any G-force mitigating vehicle design.

The next attempt at eliminating mortality employed cylinders of the same size, except that they were coated with the compound polyurea, an elastomer with a high capacity for rapid compression and decompression in response to acceleration.² The incorporation of the polyurea-coated cylinders resulted in a reduction in the maximal acceleration to a level of 550g, which is only 19% of the load imparted in the absence of compressible cylinders and 23% of the load transmitted in the presence of uncoated cylinders. The mean jerk level of 0.76 m/sec^{-3} was also much less than that

measured with no cylinders or uncoated cylinders. Most importantly, the presence of the polyurea-coated cylinders completely eliminated mortality (Table 1).

The mitigation of under-vehicle blast-induced G force by the incorporation of polyurea-coated cylinders in the vehicle design was also associated with protection against neurobehavioral alterations. The working memory deficits observed at day 0 and at day 6 after blast exposure using uncoated cylinders were completely eliminated by substitution with polyurea-coated cylinders (Fig. 2A). More importantly, the anxiety-like behavior reflected by reduced time spent in the open arms of the Plus maze for up to at least 28 days post-blast was also fully attenuated by the presence of polyurea-coated cylinders (Fig. 2B). Mitigation by an elastomeric frame design of anxiety is particularly important, because depression and anxiety are not uncommon among warfighters and civilians who have sustained blast TBI.²⁰

In addition to testing the effects of different frame designs on neurobehavioral alterations following under-vehicle blasts, we compared the ability of these modifications to mitigate the neuropathology and neurochemical alterations that occur in this under-vehicle blast TBI model. Cerebrovascular damage is a prominent feature in both impact-induced and open-field blast models of TBI.^{8,20-22} In this study, we performed quantitative immunohistochemical measurements of markers commonly associated with vascular injury. For example, disruption of the BBB is accompanied by leakage of blood proteins through the vascular wall and into the brain parenchyma. In comparison with shams, we observed a significant, twofold increase in perivascular IgG immunoreactivity in the cortex of rats at 24 h following exposure to blast when uncoated cylinders were present within the frame of the model vehicle

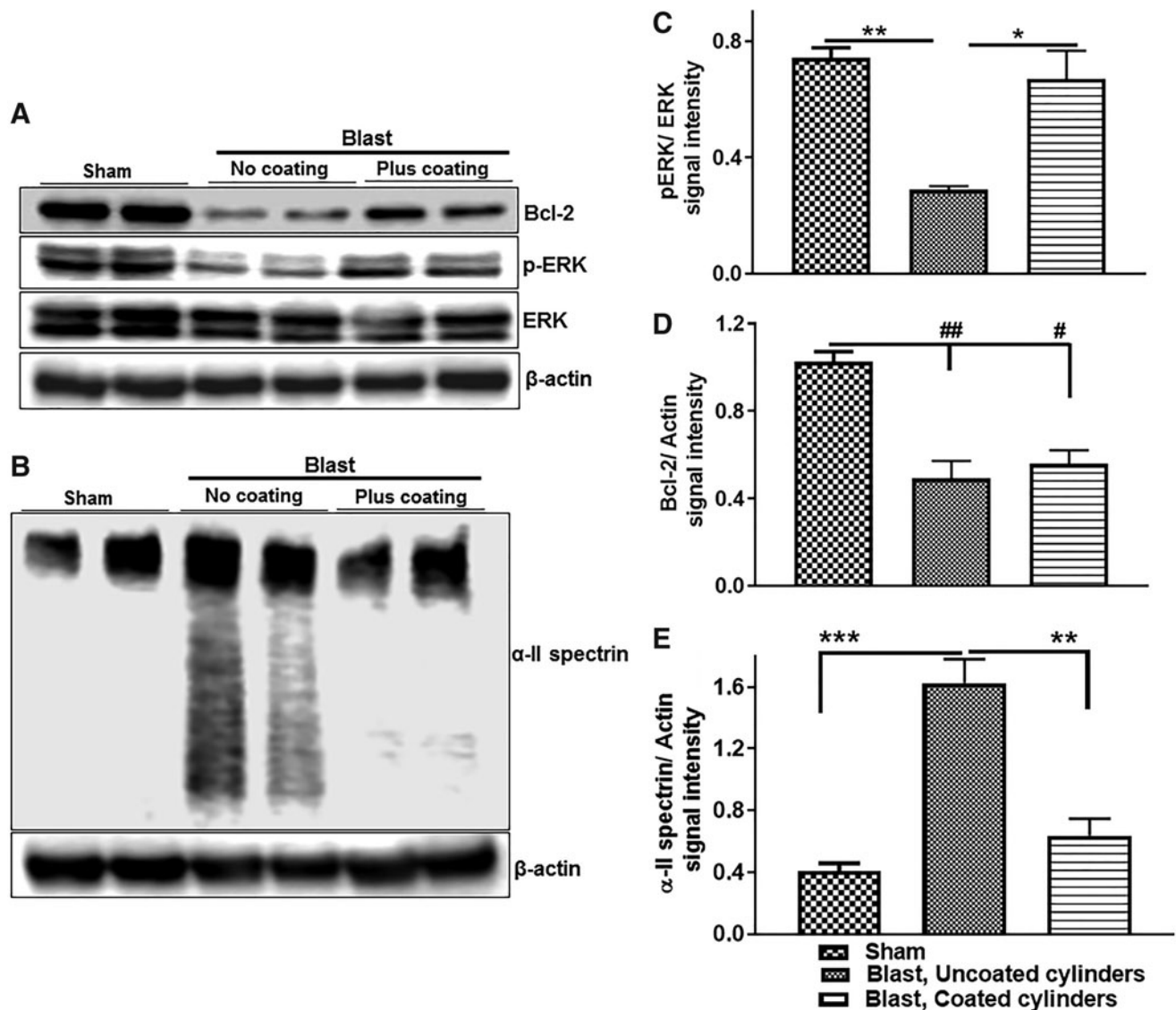


FIG. 9. Decreased expression of cell survival promoting proteins and increased expression of pro-apoptotic protein in rat hippocampus 24 h post-blast, and mitigation by the shock-absorbing hull design system. (A,B) Representative immunoblots illustrating the expression of cell survival promoting protein phospho-extracellular signal-regulated kinase (ERK), anti-apoptotic protein B-cell lymphoma 2 (Bcl-2) and proapoptotic marker α II spectrin in rat hippocampus. (C–E) Quantitation of protein band signal intensity showed, compared with sham rats, a significant decrease in phospho-ERK and Bcl-2 ($n=6$, $^{***\#\#}p < 0.01$), and a drastic increase in α II spectrin ($n=6$, $^{***}p < 0.001$) in the hippocampus of rats exposed to lethal blast intensity with no polyurea coating compared with sham rats. Rats subjected to blast with advanced hull mitigation design still showed significantly lower Bcl-2 expression levels than shams ($n=6$; $^{\#}p < 0.05$). However, the advanced hull mitigation design abrogated the deleterious effect of blast exposure on the expression phospho-ERK and α II spectrin ($n=6$; $^*p < 0.05$, and $^{**}p < 0.01$, respectively).

(Fig. 3). In contrast, the perivascular IgG immunoreactivity measured after blasts with polyurea-coated cylinders was not significantly different than that expressed in sham animals. In comparison with shams, we also observed a greater than fivefold increase in the cortical levels of ICAM-1 following blasts conducted in the presence of uncoated cylinders (Fig. 4). Increased ICAM-1 expression is often seen in other models of TBI, and facilitates the transmigration of leucocytes from the blood into the brain parenchyma.^{13,14} When polyurea-coated cylinders were substituted for uncoated cylinders, ICAM-1 levels were reduced by >50%.

Based on changes in these biomarkers of vascular injury, we anticipated that additional indicators of neuroinflammation would be observed.^{15,16} Brain tissue was therefore immunostained for F4/80, which is selective for activated microglia and macrophages. As

shown in Figure 4, a 10-fold increase in the area of immunostaining for F4/80 was measured in the cortex after blasts employing uncoated cylinders, in comparison with shams. The presence of polyurea-coated cylinders reduced the F4/80 immunoreactivity by 70%.

Neuroinflammation is often associated with neuronal death, which under some circumstances is preceded by the loss of neuronal synapses.²³ We detected a significant decrease in the pre-synaptic protein Bassoon and the post-synaptic protein Homer-1 in the hippocampal dentate gyrus and CA2 regions following blasts that generated 2350g acceleration and included the presence of uncoated cylinders in the frame design (Fig. 7). These findings taken together with reductions in other synaptic proteins reported earlier for this under-vehicle blast model⁶ provide evidence

supporting the hypothesis that loss of synapses is an important contributor to blast TBI.²⁴ The reduction in Homer and Bassoon were associated with increased cell death in the same regions, as measured by the number of cells that were cleaved caspase-3 immunopositive (Fig. 8).⁶ Proteolytic activation of caspase 3 is typically a marker of neuronal apoptosis following TBI.²⁵ Proteolysis of other proteins; for example, α ii spectrin, is also observed following TBI.^{26,27} Immunoblots revealed a fourfold increase in hippocampal α ii spectrin breakdown products at 24 h following the blasts that employed the uncoated cylinders in the vehicle frames (Fig. 9). α spectrin degradation is also implicated in the loss of synapses observed in Alzheimer's disease.²⁸ Thus, the substantial α ii spectrin breakdown observed following 2350g-associated blasts might contribute to the loss of synapses implicated by the loss of Homer and Bassoon immunoreactivity following these blasts. In contrast to the promotion of α spectrin hydrolysis, caspase 3 activation, and loss of synaptic proteins by exposure to blast-induced 2350g acceleration, all of these outcome measures were significantly reduced when the G force was reduced to 550g by the use of the polyurea-coated aluminum cylinders.

We also performed immunoblots for phospho- and dephospho-ERK and Bcl-2, which are major regulators of cell survival.^{18,29-31} Blasts that generated 2350g caused a significant reduction in the ratio of phospho-ERK to dephospho-ERK and a loss of Bcl-2 immunoreactivity. Although lowering the G force to 550g by the use of polyurea-coated cylinders eliminated the drop in pERK/ERK, the loss of Bcl-2 was surprisingly not mitigated by this frame modification.

Conclusion

The maximum peak vertical acceleration that male Sprague-Dawley rats can survive in a small-scale under-vehicle blast model is \sim 2350g. This force is roughly equivalent to 230g in a full-scale under-vehicle blast scenario, which falls within the range generated when vehicles are targeted in theater by land mines. Rats exposed to 2350g exhibit deficits in working memory for up to 6 days post-blast, and anxiety-like behavior for at least 28 days post-blast. At one day following blast exposure, the brains display evidence for cerebrovascular injury, inflammation, neuronal death, and loss of synapses. However, when the vehicle frame design is modified by the use of polyurea-coated cylinders, the peak acceleration experienced by the rats is reduced by 77%, resulting in essentially complete protection against all neurobehavioral deficits and histological evidence for brain injury. Work is in progress to further refine the elastomeric frame design, with the goal of reducing under-vehicle blast-induced G force by 90%. In addition to protecting against brain injury caused specifically by acceleration, these vehicle designs should also reduce the incidence or severity of brain injury caused by head impact within the vehicles.

Acknowledgments

We thank Ashley Moore and Julie L. Proctor for their participation in the blast experiments. This study was funded by US Army W81XWH-13-1-0016 and US Air Force FA8650-11-2-6D04.

Author Disclosure Statement

No competing financial interests exist.

References

- Hopkinson, B. (1915). *British Ordnance Board Minutes 13565*. The National Archives: Kew.
- Bonsmann, J., and Fournay, W. (2015). Mitigation of accelerations caused by blast loading utilizing polymeric-coated metallic thin-walled cylinders. *J. Dynamic Behav. Mater.* 1, 259–274.
- Tom, V.B. Pentagon: new MRAPs have been successful in saving troops' lives. *USA Today*
- Proctor, J.L., Fournay, W.L., Leiste, U.H., and Fiskum, G. (2014). Rat model of brain injury caused by under-vehicle blast-induced hyperacceleration. *J. Trauma Acute Care Surg.* 77, S83.
- Proctor, J.L., Mello, K.T., Fang, R., Puche, A.C., Rosenthal, R.E., Fournay, W.L., Leiste, U.H., and Fiskum, G. (2017). Aeromedical evacuation-relevant hypobaric worsens axonal and neurologic injury in rats following underbody blast-induced hyperacceleration. *J. Trauma Acute Care Surg.* 83, 535–542.
- Tchantchou, F., Fournay, W.L., Leiste, U.H., Vaughan, J., Rangghran, P., Puche, A., and Fiskum, G. (2017). Neuropathology and neurobehavioral alterations in a rat model of traumatic brain injury to occupants of vehicles targeted by underbody blasts. *Exp. Neurol.* 289, 9–20.
- Zhao, X., Tiwari, V., Sutton, M.A., Deng, X., Fournay, W.L., Leiste, U., Tchantchou, F., and Zhang, Y.M. (2013). Scaling of the deformation histories for clamped circular plates subjected to blast loading by buried charges. *Int. J. Impact Eng.* 54, 30, 31; 565–50; 579.
- Tchantchou, F., and Zhang, Y. (2013). Selective inhibition of alpha/beta-hydrolase domain 6 attenuates neurodegeneration, alleviates blood brain barrier breakdown, and improves functional recovery in a mouse model of traumatic brain injury. *J. Neurotrauma* 30, 565–579.
- Budde, M.D., Shah, A., McCrea, M., Cullinan, W.E., Pintar, F.A., and Stemper, B.D. (2013). Primary blast traumatic brain injury in the rat: relating diffusion tensor imaging and behavior. *Front. Neurol.* 4, 154–154.
- Tchantchou, F., Xu, Y.N., Wu, Y.J., Christen, Y., and Luo, Y. (2007). EGF 761 enhances adult hippocampal neurogenesis and phosphorylation of CREB in transgenic mouse model of Alzheimer's disease. *FASEB J.* 21, 2400–2408.
- Ippolito, D.M., and Eroglu, C. (2010). Quantifying synapses: an immunocytochemistry-based assay to quantify synapse number. *J. Vis. Exp.* (45). pii: 2270.
- McKinstry, S.U., Karadeniz, Y.B., Worthington, A.K., Hayrapetyan, V.Y., Ozlu, M.I., Serafin-Molina, K., Risher, W.C., Ustunkaya, T., Dragatsis, I., Zeitlin, S., Yin, H.H., and Eroglu, C. (2014). Huntingtin is required for normal excitatory synapse development in cortical and striatal circuits. *J. Neurosci.* 34, 9455–9472.
- Di Lorenzo, A., Manes, T.D., Davalos, A., Wright, P.L., and Sessa, W.C. (2011). Endothelial reticulon-4B (Nogo-B) regulates ICAM-1-mediated leukocyte transmigration and acute inflammation. *Blood* 117, 2284–2295.
- Liu, Y., Shaw, S.K., Ma, S., Yang, L., Lusinskas, F.W., and Parkos, C.A. (2004). Regulation of leukocyte transmigration: cell surface interactions and signaling events. *J. Immunol.* 172, 7–13.
- Corps, K.N., Roth, T.L., and McGavern, D.B. (2015). Inflammation and neuroprotection in traumatic brain injury. *JAMA Neurol.* 72, 355–362.
- Loane, D.J., and Byrnes, K.R. (2010). Review article: role of microglia in neurotrauma. *Neurotherapeutics* 7, 366–377.
- Gao, X., Deng, P., Zao, C.X., and Chen, J. (2011). Moderate traumatic brain injury causes acute dendritic and synaptic degeneration in the hippocampal dentate gyrus. *PLoS One* 6, e24566.
- Tchantchou, F., Tucker, L.B., Fu, A.H., Bluett, R.J., McCabe, J.T., Patel, S., and Zhang, Y. (2014). The fatty acid amide hydrolase inhibitor PF-3845 promotes neuronal survival, attenuates inflammation and improves functional recovery in mice with traumatic brain injury. *Neuropharmacology* 85, 427–439.
- Chabai, A.J. (1965). On scaling dimensions of craters produced by buried explosives. *J. Geophys. Res.* 70, 5075.
- Agoston, D.V., and Kamnakh, A. (2015). Modeling the neurobehavioral consequences of blast-induced traumatic brain injury spectrum disorder and identifying related biomarkers, in: *Brain Neurotrauma: Molecular, Neuropsychological, and Rehabilitation Aspects*. F.H. Kobeissy (ed.). Taylor & Francis Group, LLC: Boca Raton.
- Tanno, H., Nockels, R.P., Pitts, L.H., and Noble, L.J. (1992). Breakdown of the blood-brain barrier after fluid percussion brain injury in

- the rat: Part 2: effect of hypoxia on permeability to plasma proteins. *J. Neurotrauma* 9, 335–347.
22. Kabu, S., Jaffer, H., Petro, M., Dudzinski, D., Stewart, D., Courtney, A., Courtney, M., and Labhasetwar, V. (2015). Blast-associated shock waves result in increased brain vascular leakage and elevated ROS levels in a rat model of traumatic brain injury. *PLoS One* 10, e0127971.
 23. Hilton, K.J., Cunningham, C., Reynolds, R.A., Perry, V.H. (2013). Early hippocampal synaptic loss precedes neuronal loss and associates with early behavioural deficits in three distinct strains of prion disease. *PLoS One* 8, e68062.
 24. Przekwas, A., Somayaji, M.R., and Gupta, R.K. (2016). Synaptic mechanisms of blast-induced brain injury. *Front. Neurol.* 7, 2.
 25. Clark, R.S.B., Kochanek, P.M., Watkins, S.C., Chen, M., Dixon, C.E., Seidberg, N.A., Melick, J., Loeffert, J.E., Nathaniel, P.D., Jin, K.L., and Graham, S.H. (2000). Caspase-3 mediated neuronal death after traumatic brain injury in rats. *J. Neurochem.* 74, 740–753.
 26. Schober, M.E., Requena, D.F., Davis, L.J., Metzger, R.R., Bennett, K.S., Morita, D., Niedzwecki, C., Yang, Z., and Wang, K.K.W. (2014). Research report: alpha ii spectrin breakdown products in immature Sprague Dawley rat hippocampus and cortex after traumatic brain injury. *Brain Res.* 1574, 105–112.
 27. Pike, B.R., Flint, J., Dutta, S., Johnson, E., Wang, K.K., and Hayes, R.L. (2001). Accumulation of non-erythroid alpha II-spectrin and calpain-cleaved alpha II-spectrin breakdown products in cerebrospinal fluid after traumatic brain injury in rats. *J. Neurochem.* 78, 1297–1306.
 28. Kurbatskaya, K., Phillips, E.C., Croft, C.L., Dentoni, G., Hughes, M.M., Wade, M.A., Al-Sarraj, S., Troakes, C., O'Neill, M.J., and Perez-Nievas, B.G. (2016). Upregulation of calpain activity precedes tau phosphorylation and loss of synaptic proteins in Alzheimer's disease brain. *Acta Neuropathol. Commun.* 4, 34.
 29. Atkins, C.M., Falo, M.C., Alonso, O.F., Bramlett, H.M., and Dietrich, W.D. (2009). Deficits in ERK and CREB activation in the hippocampus after traumatic brain injury. *Neurosci. Lett.* 459, 52–56.
 30. Kuo, J.R., Cheng, Y.H., Chen, Y.S., Chio, C.C., and Gean, P.W. (2013). Involvement of extracellular signal regulated kinases in traumatic brain injury-induced depression in rodents. *J. Neurotrauma* 30, 1223–1231.
 31. Subramanian, M., and Shaha, C. (2007). Up-regulation of Bcl-2 through ERK phosphorylation is associated with human macrophage survival in an estrogen microenvironment. *J. Immunol.* 179, 2330–2338.

Address correspondence to:

Gary Fiskum, PhD

University of Maryland School of Medicine

685 W. Baltimore Street, MSTF 5.34

Baltimore, MD 21201

E-mail: gfishum@som.umaryland.edu